Experiment Study on the Impact Limit of Basalt/Aramid Stuffed Whipple Shields

Jiangkai Wu[1,2(✉)], Runqiang Chi[1(✉)], Guotong Sun[2(✉)], Zengyao Han[3(✉)], Baojun Pang[1(✉)], and Shigui Zheng[2(✉)]

[1] School of Astronautics, Harbin Institute of Technology, Harbin 150001, China
wjkl958@216.com, {chirq,pangbj}@hit.edu.cn
[2] Beijing Institute of Spacecraft System Engineering, Beijing 100094, China
616823537@qq.com, 448035791@qq.com
[3] China Academy of Space Technology, Beijing 100094, China
hzy@163.com

Abstract. The impact limit equation is an important basis for risk assessment and the optimal design of stuffed Whipple shields. The internationally commonly used NASA impact limit equations and curves for Nextel/Kevlar stuffed Whipple shields (hereinafter referred to as improved NASA equations) cannot be accurately applied to the protection performance predicts of Chinese basalt/aramid fiber stuffed Whipple shields. This paper studies the hypersonic impact damage characteristics of the basalt/aramid fiber stuffed Whipple shields of the China certain large manned spacecraft. Based on the test data of three types of stuffed Whipple shields, two methods are adopted to modify the parameters of the NASA equations impact limit equation, and it is determined that it is suitable for The impact limit equations and parameters of domestic stuffed Whipple shields. The improved impact limit equations can provide higher prediction accuracy, and provide a reference for the engineering optimization design of shields and the risk assessment of on-orbit missions.

Keywords: Stuffed whipple shields · Impact limit equation · Impact limit curve · Critical velocity

1 Introduction

Space debris and micro-meteoroids (Micro-Meteoroid & Orbital Debris, hereinafter referred to as MMOD) pose serious threat to the safe operation of spacecraft, especially manned spacecraft. MMOD impact affects the safety of astronauts and directly affects the success or failure of missions [1]. In order to improve the protection of spacecraft against MMOD, stuffed structures, multi-impact shielding structures, and mesh dual-wall shielding structures have been developed. Various shielding structures, as well as impact limit equations and curves [2], among which the stuffed Whipple shields has increased the protective capacity due to the addition of high modulus and high-strength filling layer materials, with small increase in weight. Stuffed Whipple shields get more and more engineering applications, the high-risk areas of each cabin of the International Space Station basically adopt stuffed Whipple shields, and the filling materials include Nextel ceramic fiber layers and Kevlar high-strength fiber layers [3, 4].

J. Sun et al. (Eds.): *Signal and Information Processing, Networking and Computers*, LNEE 917, pp. 206–215, 2023.
https://doi.org/10.1007/978-981-19-3387-5_24

China manned space project is steadily advancing, For the reliable, safe and ten years long-life operation of the China certain spacecraft in orbit, A large number of protective structure design and verification work has been carried out for the manned project, and finally three types of stuffed Whipple shields have been selected. The filling layers is selected as three layers of basalt Fiber cloth and three layers aramid fiber cloth, basalt fiber cloth on the outer layers, and aramid fiber cloth on the inner layers [5]. The test results show that the impact limit equation and curve of the NASA equations commonly used in the world cannot be accurately applied to the stuffed shield structures of the China certain spacecraft due to the strength characteristics of aluminum alloy and the difference of the filling layer materials. The protective performance of the structure predicts that the NASA equations predicts that the result is too conservative in the low-velocity zone, behave as the ballistic limit diameter predict result is much smaller than the test result, while the predictive result in the high-velocity zone is too aggressive, indicating that the result is much higher than the test result [6].

Based on the analysis of the impact characteristics of the three types of stuffed Whipple shields, and according to the results of the impact test in the mid-velocity zone, this paper first established the impact limit equation in the mid-velocity zone, and based on the modified NASA equations in the low-velocity zone and high-velocity zone equations. The velocity threshold of low-velocity zone to mid-velocity zone and the velocity threshold of mid-velocity zone to high-velocity zone have determined the impact limit equations and parameters applicable to domestic stuffed Whipple shields, which provide a reference for the risk assessment of engineers and the optimization of shielding structures.

2 Whipple Shields Stuffed with Basalt/aramid and Impact Test

2.1 Protective Mechanism for Stuffed Whipple Shields

The stuffed Whipple shields achieves a better protection performance under the condition of a smaller protection distance, At present, stuffed Whipple shields has been successfully applied to manned spacecraft such as the International Space Station. According to ground test results, the stuffed Whipple shields has better protection performance than the Whipple shielding structure, and can greatly improve the MMOD protection capability of the orbiting spacecraft [7, 8].

In the early demonstration stage of the China manned space project, more than one dozen materials such as carbon fiber fabric, glass fiber fabric, Kevlar fiber fabric, silica fiber fabric, basalt fiber fabric, silicon carbide fiber fabric, silicon carbide blanket, PBO, etc. Considering the protective performance of the high-velocity zone, production cost, technology, and other factors, the engineers finally selected the basalt and aramid stuffed Whipple shields, and the filling layer selected three layers of basalt fiber for outer and three layers of aramid fiber for inner. The stuffed Whipple shields parameters are shown in Table 1 [5, 8].

Table 1. Parameters of three types of shielding structure for China large spacecraft.

No	Bumper material	Bumper thickness/mm	Filling material	Rear wall material	Rear wall thickness/mm	S1/mm	S2/mm
SW1	5A06	1.0	One Anti-Atomic Oxygen Film, three layers of basalt, layers of aramid, thermal multilayer	5A06	2.5	17.5	100
SW2	3A12	0.8			2.5	17.5	60
SW3	3A12	0.8			3.5	21.5	100

Where S1 represents the distance between the infill layer and the rear wall and S2 represents the distance between the infill layer and the bumper.

2.2 Ultrahigh Velocity Impact Test

Utilizing the FD-18A and FD-18C hypervelocity impact targets of the Institute of Supervelocity Aerodynamics of China Aerodynamics Research and Development Center, and equipped with 7.6 mm caliber and 16 mm caliber secondary light gas guns, as shown in Fig. 1, the completion Impact three type tests of stuffed Whipple shields for certain China spacecraft.

a. FD-18A hypervelocity impact target

b. FD-18C hypervelocity impact target

Fig. 1. FD-18A and FD-18C hypervelocity impact targets.

By adding a 1 mm thick 5A06 aluminum alloy plate as an witness plate 50 mm away behind the rear wall, impact test pieces were formed, as shown in Fig. 2, with three layers of basalt fiber and three layers of aramid fiber, with area density 0.096 g/cm^2 and 0.06 g/cm^2. The anti-atomic oxygen film and thermal control multi-layer density is 0.05 g/cm^2, the projectile is made of 2A12 aluminum alloy material standard spherical projectile [8].

For the three types of shielding configurations, 8-round, 7-round and 7-round impact tests were carried out. Based on the analysis of the validity of the data, the results of the test with impact angle of 0° are shown in Table 2. In these tests, the protective effect of the stuffed Whipple shields is evaluated based on whether the rear wall is perforated or peeled off: if the rear wall is not perforated or peeled off, the protection is effective; if the rear wall is perforated, peeled off or cracked, the protection is fail [8–10].

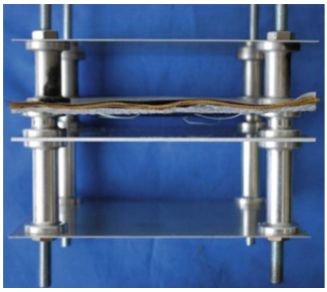

Fig. 2. Basalt aramid fiber filling shielding structure test piece.

Table 2. Test results for SW1, SW2 and SW3 shielding configuration.

Sample number	Projectile diameter/mm	Projectile mass/g	Impact velocity/km/s	Penetrate	Sample Number	Projectile diameter/mm	Projectile mass/g	Impact velocity/km/s	Penetrate
SW1–1	5.00	0.1823	3.09	Y	SW2–7	6.00	0.3183	6.715	N
SW1–2	4.75	0.1554	3.04	Y	SW2–8	6.50	0.4013	6.512	N
SW1–7	4.50	0.1333	3.149	Y	SW2–9	7.00	0.5005	6.364	Y
SW1–9	4.25	0.1118	3.072	Y	SW2–10	6.75	0.4496	6.571	Y
SW1–10	4.00	0.0929	3.028	N	SW3–1	4.50	0.1338	2.957	Y
SW1–11	8.00	0.7467	6.463	N	SW3–2	4.75	0.1555	3.176	Y
SW1–12	8.50	0.8968	6.326	Y	SW3–3	5.00	0.1822	3.072	Y
SW1–16	8.25	0.8193	6.536	N	SW3–7	9.00	1.0605	6.391	Y
SW2–1	4.25	0.1113	3.03	Y	SW3–8	8.50	0.897	6.398	N
SW2–2	3.75	0.0753	3.156	N	SW3–9	8.75	0.9754	6.501	Y
SW2–3	4.00	0.0925	3.165	N	SW3–12	4.25	0.1113	3.063	N

2.3 Damage Characteristic Analysis of the Shield

The projectiles with an impact velocity near 3 km/s penetrate the bumper and form petal-shaped flanges on the front and back openings. Only the material near the impact point of the projectile and the bumper is partially melted, and the diameter of the bumper n perforation is greater than the diameter of the projectile indicates that the projectile is broken and melted when it hits the shield. The volume of the projectile and the fragment cloud of the shield expands, the energy spreads, and further hits the filling layer. The filling layer forms a large damage area, the outer side is a circular area damage, and there are many small holes scattered around, the diameter is about 1 to 5 times the diameter of the perforation of the shield under low-velocity impact, typical damage is shown in Fig. 3.

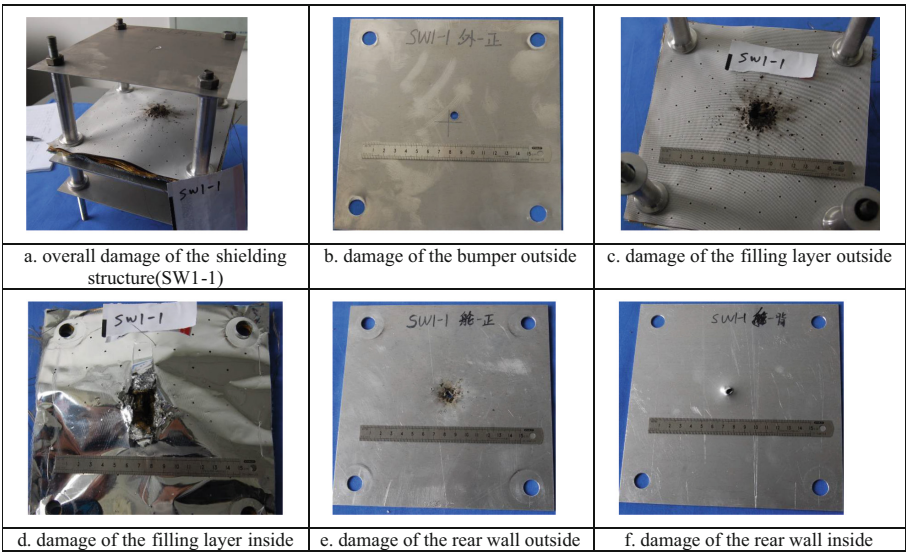

a. overall damage of the shielding structure(SW1-1) | b. damage of the bumper outside | c. damage of the filling layer outside

d. damage of the filling layer inside | e. damage of the rear wall outside | f. damage of the rear wall inside

Fig. 3. Damage of shielding structure under low-velocity impact near 3 km/s.

3 Research on Impact Limit Equation and Parameters

The impact limit equation is an important basis for risk assessment and protection structure optimization design. The NASA equations are fitted based on a large amount of test dates [2, 11]. The critical velocity VL in the crushing zone and the critical velocity VH in the crushing zone and the gasification zone are different in two velocity points, which indicate low accuracy for the impact limit of the China stuffed Whipple shields. In this paper, two methods are adopted to modify the parameters of the NASA equations, and the impact limit equations suitable for stuffed Whipple shields are obtained, which provides a reference for the subsequent engineering evaluation of the protective capacity.

1) Keeping the form of NASA equations unchanged, using the multiple linear regression and genetic algorithm methods, based on the China spacecraft's three types of protective structure impact test dates, the coefficients of the NASA equations were corrected, and the impact limit equation of the stuffed Whipple shields suitable for the China certain spacecraft was obtained.
2) Make full use of the NASA equations in the ballistic zone and the gasification zone to predict high accuracy, and only modify the impact limit equation in the medium-velocity zone, obtain two critical impact velocity thresholds in the low-velocity zone and high-velocity zone, and obtain the full velocity for the domestic protective structure Zone impact limit equation.

3.1 NASA Nextel/Kevlar Stuffed Whipple Shields Equations

There are many parameters influencing the impact limit equation of the stuffed Whipple shields. In 2003, referring to the impact limit equation of the Whipple protective structure, Christiansen et al. proposed the Nextel/Kevlar stuffed Whipple shields impact limit equation for the International Space Station through a large amount of ground tests [2, 11].

1) For $V \leq 2.6/(\cos\theta)^{0.5}$

$$d_c = 2.35 \times (t_w(\sigma/275.8)^{0.5} + 0.37m_b) \times \rho_p^{-0.5} \times V^{-2/3} \times (\cos\theta)^{-0.75} \quad (1)$$

where m_b——Total areal density of the bumper and the filling layer, in g/cm^2

2) For $V \geq 6.5/(\cos\theta)^{0.75}$

$$d_c = 0.6 \times (tw \times \rho w)^{1/3} \times \rho_p^{-1/3} \times (\sigma/275.8)^{1/6} \times S^{2/3} \times V^{-1/3} \times (\cos\theta)^{-0.5} \quad (2)$$

3) For $2.6/(\cos\theta)^{0.5} < V < 6.5/(\cos\theta)^{0.75}$

$$d_c = 1.243\left(t_w \times \left(\frac{\sigma}{275.8}\right)^{0.5} + 0.37m_b\right) \times \rho_p^{-0.5} \times (\cos\theta)^{-1} \times (6.5/(\cos\theta)^{0.75} - V)/(6.5/(\cos\theta)^{0.75} - 2.6/(\cos\theta)^{0.5}) + 0.321(t_w \times \rho_w)^{\frac{1}{3}} \times \rho_p^{-\frac{1}{3}} \times \left(\frac{\sigma}{275.8}\right)^{\frac{1}{6}} \times S^{\frac{2}{3}} \times (\cos\theta)^{-0.25} \times (V - 2.6/(\cos\theta)^{0.5})/(6.5/(\cos\theta)^{0.75} - 2.6/(\cos\theta)^{0.5}) \quad (3)$$

Constant: 2.35 ($g^{1/2}cm^{-3/2}km^{-2/3}s^{-2/3}$), 275.8 (MPa), 0.37 ($g^{-1}cm^3$), 1.243 ($g^{1/2}cm^{-3/2}$), 275.8 (MPa), 0.37 ($g^{-1}cm^3$), 6.5 (km/s), 2.6 (km/s). 0.6 ($km^{1/3}s^{-1/3}$), 275.8 (MPa); The rest are dimensionless constants.

d_c refer to Critical projectile diameter, (cm), t_w refer to rear wall thickness, (cm), ρ_w refer to density of the bumper, (g/cm^3), ρ_P refer to density of the projectile, (g/cm^3), σ refer to Yield strength of rear wall, (MPa), S refer to distance between the bumper and rear wall, (cm), V refer to impact velocity of the projectile, (km/s), m_b refer to Total areal density of the bumper and the filling layer (g/cm^2), θ refer to impact angle, (degree).

Using the NASA equations to predict the impact limit of the three types of stuffed Whipple shields, as shown in Fig. 4, compared with the test results, it is shown that close to the low-velocity zone, the prediction results are conservative. For example, for SW1, when the impact velocity is 3 km/s, It indicates that the impact limit diameter of the shielding structures is only 0.38 cm, but the test result reaches 0.45 cm; close to the high-velocity zone, the result indicates that the result is biased toward advancing.

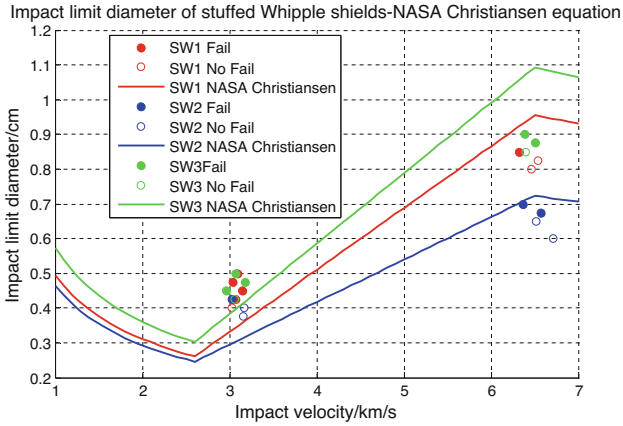

Fig. 4. Prediction of NASA equations and the comparison with the test dates.

3.2 Parameter Modification of Impact Limit Equation

Analyze the NASA equations, in the ballistic zone $(V \leq 2.6/(\cos\theta)^{0.5})$, $a1 \times tw \times (sigma/275.8)^{0.5} + a2 \times mb \times V^{a3}$ is variable, thus, let $T_1 = a1 \times tw \times (sigma/275.8)^{0.5} + a2 \times mb \times V^{a3}$, In the gasification zone $(V \geq 6.5/(\cos\theta)^{0.75})$, $(V \geq 6.5/(\cos\theta)^{0.75})$ is variable, thus, let $T_2 = (tw \times \rho w)^{a4} \times S^{a5} \times V^{a6}$. Thus, we can Rewrite the NASA equations as:

1) For

$$V \leq 2.6/(\cos\theta)^{0.5}, d_c = 2.35 \times \rho_p^{-0.5} \times T_1 \times (\cos\theta)^{-0.75} \tag{4}$$

2) for

$$V \geq 6.5/(\cos\theta)^{0.75}, d_c = 0.6 \times \rho_p^{-1/3} \times (sigma/275.8)^{1/6} \times T_2 \times (\cos\theta)^{-0.5} \tag{5}$$

Using genetic optimization algorithm, aiming to minimize the error between the predicted result and the shielding structure test dates at a given velocity, and using the 0° impact angle test dates, the T_1 and T_2 values of the three types of shielding structures are shown in Table 3.

Table 3. Parameters for three types of shielding structures.

Shielding structures	T_1	T_2
SW1	0.33	4.28
SW2	0.33	3.196
SW3	0.3423	4.36

Table 4. Parameters for impact limit equation.

a1	a2	a3	a4	a5	a6
0.1203	0.792	−0.76	0.08	0.575	−1/3

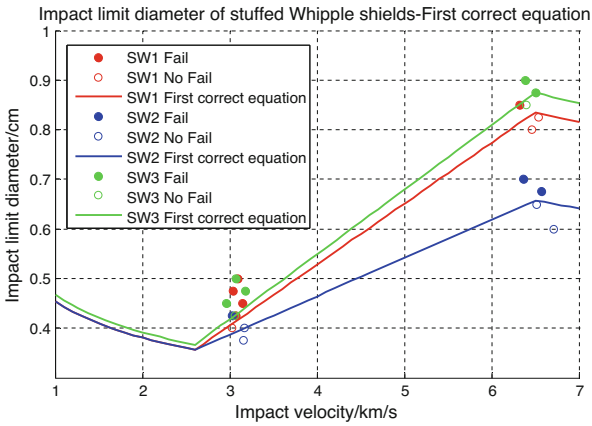

Fig. 5. Modified impact limit equation prediction and comparison with experimental dates.

Using multiple linear regression equations, the undetermined parameters of different shielding structures are shown in Table 4.

The modified impact limit equation parameters are used to predict the impact limit of the shielding structures the China certain spacecraft, As shown in Fig. 5. SW2 and SW3 indicate that the curve just crosses the non-breakdown point near 3.1 km/s, and the results are conservative. The accuracy rate reached 100%, which can well reflect the impact limit capability of the shielding structure.

3.3 Impact Limit Velocity Threshold Correction

The impact limit equation for the crushing zone is usually obtained by interpolation of the impact limit diameters at the critical velocities of VL and VH on the basis of the impact limit equations of the ballistic section and the vaporization section. It is a linear equation of the first order, which can be established as $d_c = c_1 + c_2 \times (V - V_L)$. Using the test dates with an impact angle of 0 ° and using the median theorem to determine the impact limit at the test impact velocity, the impact limit equations for the broken

Table 5. VL and VH values for three types shielding structure.

Shielding structures	VL	VH
SW1	2.18	7.10
SW2	1.80	6.98
SW3	2.25	7.82

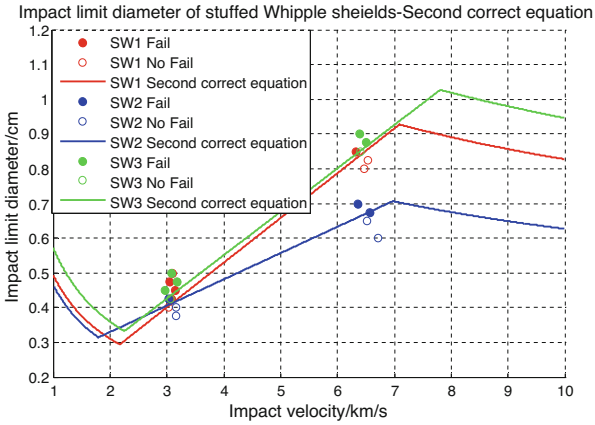

Fig. 6. Modification of impact limit velocity threshold and comparison with test results.

zone of three types of protective structures are obtained for SW1, $d_c = 0.0132 + 0.1288 \times V$; for SW2, $d_c = 0.1755 + 0.0758 \times V$; for SW3, $d_c = 0.05 + 0.1250 \times V$; Using the modified impact limit equation of the crushing zone to intersect the ballistic section and vaporization section equations of the NASA equations, three types of shielding structures VL and VH are obtained as shown in Table 5.

The three velocity zone impact limit equations are combined, and the impact limit of the China spacecraft's shielding structure is predicted. As shown in Fig. 6, the predict success rate reached 100%.

4 Conclusion

In this paper, the ultra-high-velocity impact damage characteristics of the basalt/aramid-filled shielding structure of the China spacecraft are studied, and the NASA equations is modified based on the experimental dates, and the impact limit equation and parameters suitable for the stuffed Whipple shields are determined, and the improved impact limit equation is determined that, It can provide higher prediction accuracy and provide a reference for the optimization of engineering protection structure design and the risk assessment of on-orbit mission.

References

1. Wu, J.K., et al.: Development of risk assessment system for spacecraft under MMOD impact and the enlightenment. Spacecraft Environment Engineering **37**(6), 531–539 (2020)
2. Ryan, S., Christiansen, E.L.: Micrometeoroid and Orbital Debris (MMOD) Shield Ballistic Limit Analysis Program: NASA JSC. NASA JSC TM-2009–214789 (2009)
3. Christiansen, E.L., Nagy, K., Lear, D.M., Prior, T.G.: Space station MMOD shielding. Acta Astronaut **65**(7–8), 921–929 (2009). https://doi.org/10.1016/j.actaastro.2008.01.046

4. Christiansen, E.L.: Enhanced meteoroid and orbital debris shielding. Int. J. Impact Eng **17**, 217–228 (1995)
5. Yan, J., Zheng, S.: A research on middle layer impact characteristic of stuffed whipple shields, manned. Spaceflight **19**(1), 10–14 (2013)
6. Purzar, R., et al.: A stuffed Whipple shield for the Chinese space station. Int. J. Impact Eng. **132**, 103304 (2019). https://doi.org/10.1016/j.ijimpeng.2019.05.018
7. Jia, G., Ha, Y., Pang, B., Guan, G., Zu, S.: Ballistic limit and damage properties of basalt/Kevlar stuffed shield. Explos Shock Waves **36**(4), 433–440 (2016). https://doi.org/10.11883/1001-1455(2016)04-0433-08 (in Chinese)
8. Zheng, S.-G., Zhang, S., Gong, W.-W.: Impact characterization of stuffed whipple for space station. Space Debris Research **18**(1), 41 ~ 47 (2018)
9. Zheng, S., Yan, J., Weiwei, G.: Impact characterization of stuffed whipple for china space station. In: Flohrer, T., Schmitz, F. (eds.) Proceedings of the 7th European Conference on Space Debris. Darmstadt, ESA Space Debris Office (2017)
10. Zheng, S., Yan, J., Shan, L., Jiang, C.: Research on shield for space station from meteoroid and orbital debris. In: Proceedings of the 64th International Astronautical Congress. Beijing, China (2013). IAC-13,A6,3,4,x17523
11. Christiansen, E.L., et al.: Handbook for designing MMOD protection: NASA Johnson Space Center (2009). NASA/TM-2009–214785